Pure & Appl. Chem., Vol. 64, No. 11, pp. 1589–1602, 1992.
Printed in Great Britain.
© 1992 IUPAC

Lattice models of amphiphilic assembly

K. A. DAWSON
Department of Chemistry, University of California, Berkeley, CA 94720, USA

ABSTRACT
We discuss recent attempts to model amphiphilic self-assembly phenomena by using lattice models. These are an attempt to represent mesoscopic length-scale structure and long time-scale dynamics of such complex fluids. We extract an effective Landau theory from the lattice model and under renormalization it is found to represent the microemulsion region of the lattice model quite well. The coefficient of the gradient-squared term in the Landau theory is negative and the implications of this for structure, interfacial properties and dynamics are discussed.

1. INTRODUCTION

In these lecture notes we shall be discussing a particular type of very complex fluid that originates from *self-assembly*.[1] Such fluids are formed by mixing amphiphile[2] with hydrophilic (e.g., water) and perhaps some hydrophobic (alkanes or "oil") material. The amphiphilic molecules assemble into aggregates to avoid exposing their hydrohobic regions to water and their hydrophilic region to oil. In addition the amphiphile aggregates may acquire additional stability by correct orientation of the amphiphiles with respect to each other. In any case, the energy scales keeping the assembly in a given form are small, being merely of order kT per molecule. This means that the time a given molecule spends in a given aggregate may be very small and for many purposes it is not appropriate to think of such a cluster as a geometrical object that is closed with respect to mass transfer[3] but rather as a rapidly fluctuating object with respect to density. Furthermore, the phase-transitions between phases with different geometries may involve energies that are much smaller than the assembly energy, and originate in quite subtle changes of the geometry or connectivity of the supramolecular aggregates.

In attempting to construct models of these materials it is worth pointing out that they exhibit few truly universal features. Rather they present interesting and important generic properties and trends that we will seek to understand in a unified manner. There is also the further practical aspect that many of the phenomena, though they originate in self-assembly at the microscopic level, are actually mediated by long, but not diverging, length-scales. For this reason it is convenient to construct a model that is computationally tractable, thereby facilitating the study of these various trends, but that is reducible to a more compact coarse-grained Hamiltonian whenever one seeks to study universal features via renormalization calculations.

There are some further considerations to be taken into account when formulating the model. Thus, if one is to understand a range of amphiphilic behavior, there should be sufficient flexibility to represent the effect of geometric fluctuations of self-assembled structures, as well as fluctuations causing the break-up of the phase. This indicates that the simplest possible formulation may be that of a lattice model.

Many of the comments just made refer quite generally to self-assembled fluids whether they be lytotropic liquid crystals, micelles or microemulsion. We shall now turn to a discussion of the experimental observations for three-component mixtures of oil, water and amphiphile.[4]

2. SOME EXPERIMENTAL OBSERVATIONS AND PHENEMENOLOGY

Upon mixing oil, water, and a little surfactant one often finds a macroscopic thermodynamically stable phase named microemulsion that possesses some quite remarkable properties. Microemulsion has found application in a number of developing technologies such as enhanced oil-recovery and clean-up, catalytic systems and synthetic blood substitutes. Some of the prominent experimental observations associated with these fluids are described below. They may also be encapsulated in the three-phase triangle, Figure 1.[5]

As a function of the concentration of amphiphile, temperature and brine one finds a phase-equilibrium between microemulsion, oil-in-water and water-in-oil micellar phases. In some cases the middle microemulsion phase in this equilibrium is replaced by a lamellar liquid-crystalline phase. As one proceeds to the oil-rich or water-rich regions of the phase-diagram the three-phase equilibrium collapses to an oil-microemulsion or water-microemulsion two-phase equilibrium via critical-end-points of, respectively, the water and

*This represents part of the text of a lecture given at the Seventh International Conference on Surface and Colloid Science, Compiegne, France. In that same year some of this material was presented at the NATO Summer School held in Aquafredda di Maratea, Italy.

microemulsion or oil and microemulsion. This three-phase coexistence, often named the Winsor III state, is of particular interest both from the viewpoint of basic statistical mechanics and for its technological importance.

Thus, in this region of the phase-diagram the middle microemulsion phase is often opalescent and its interfacial tensions with the coexisting phases are ultra-low leading many to suppose that the liquid is near-critical. However, the volume-fractions of the various components in the three phases may differ significantly and, characteristically, the microemulsion does not wet the oil-water interface. Both of these observations seem to indicate the properties of the middle-phase may not be ascribed solely to a proximate critical point. Furthermore, the interfacial tension data in the three-phase region exhibit a rather characteristic and interesting pattern between the two critical end-points. The tension between a pair of incipient critical phases naturally decreases monotonically, whilst that between the other pair rises monotonically. On the other hand, the oil-water tension actually exhibits a minimum between the two critical end-points, a phenomenon that has long been used as the criterion of an optimal microemulsion. In that region of three-phase equilibrium where the oil-water tension is a minimum, the microemulsion contains almost equal volume-fractions of oil and water and a fairly small amount (between 10-20% with respect to volume) of amphiphile. It is bicontinuous in the sense that it conducts electricity and the apolar molecular diffusivity is high.

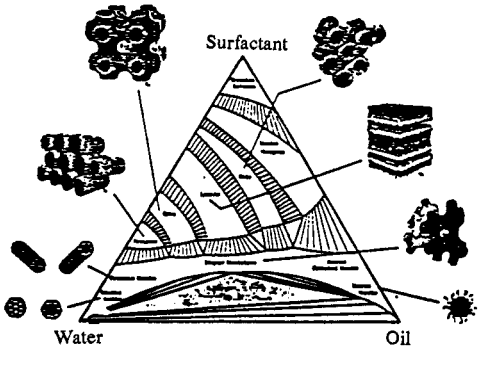

Figure 1. Schematic phase-diagram of three-component oil-water-amphiphile mixture (see reference 5).

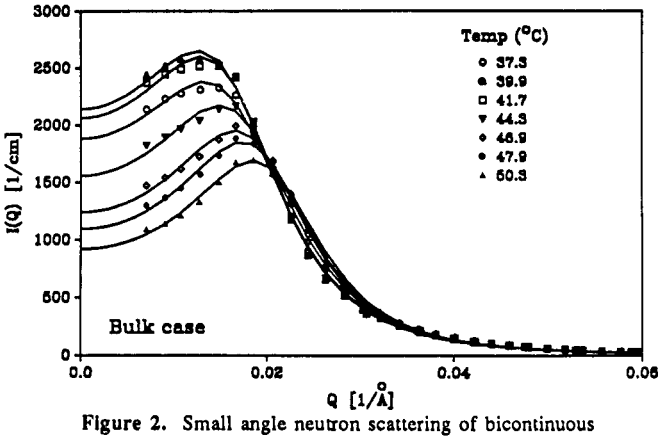

Figure 2. Small angle neutron scattering of bicontinuous microemulsion (see reference 6).

Recently a number of scattering studies of this bicontinuous phase have been undertaken. These include small-angle neutron-scattering (S.A.N.S), light scattering, and also freeze-fracture electron microscopy. In particular, the S.A.N.S studies produce a peak in the scattering intensity at small wave-numbers, an observation that is consistent with the presence of two relatively long length-scales in the microemulsion. The ratio between these lengths appears to be fairly constant in the bicontinuous region, and is approximately equal to four. This observation has been made in the literature by Widom and further elucidated by Chen. It is also observed that, with increasing amphiphile concentration and changing temperature, the peak in the S.A.N.S intensity shifts to shorter wave-lengths (see Figure 2).

Finally we note that the phase-diagram also possesses a one-phase-region spanning the oil-in-water, bicontinuous and water-in-oil phases. It is believed that, typically, this single-phase corridor permits one to accomplish phase-inversion without undergoing a phase-transition. These, then, are some of the prominent aspects of the phase-diagrams of mixtures of amphiphile, oil and water where one has relatively small amounts of amphiphile. We note in passing that, at higher amphiphile concentrations, one finds various liquid-crystalline phases.

The purpose of the present discussion is to show that all of these features are present in a relatively simple lattice model. Within this model it is also possible to explain the origins of these phenomena, and to see that the puzzling experimental observations are, indeed, entirely consistent with one another.

We now turn to the discussion of dynamical and non-equilibrium studies of self-assembled materials. The measurements of dynamical or non-equilibrium properties of these systems have received less attention, though they are also important scientifically and industrially. There has however been a recent renewal of interest in the rheological properties of amphiphilic systems and complex supramolecular fluids generally. One reason for the limited progress that has been made in modelling these fluids is that, unlike simple fluids that are composed of intact atoms or molecules that interact through weak molecular forces, the basic interacting unit in a self-assembled fluid may change under small perturbations. Such units cannot therefore be assumed to maintain their integrity for the purposes of theoretical description. For example, in attempting to describe even the bulk viscosity of the bicontinuous phase one realizes that an elementary model of molecular viscosity would not be appropriate since the flexibility and cohesiveness of the amphiphilic film must also be important factors. Indeed, the description of the bulk viscosity of microemulsion throughout the phase-diagram is quite an interesting problem. On passing across the $2\underline{3}\overline{2}$ progression[5,6] there are two peaks in the viscosity of the microemulsion that are somewhat loosely correlated with the rise in conductivity and apolar molecular diffusivity. Between these two

peaks the viscosity is surprisingly low (on the order of one centipoise), especially given the conventional picture of the bicontinuous structure. We note that throughout most of the microemulsion region the viscosity is essentially Newtonian, though it is shear birefringent. There is a rather strong correlation between the minimum in viscosity and optimal salinity. This overall pattern of viscosities is not well understood, and at present there exists no theory to describe the situation. Heuristically one might argue that the minimum in the viscosity curve arises because the bicontinuous state readily heals any tears in the amphiphilic film caused by momentum transfer from a disturbance. This might cause the transverse momentum currents to decorrelate quite rapidly and result in low viscosity. Certainly the optimal microemulsion is a rapidly fluctuating state and this may mean that time-scales for healing are relatively short. The origin of the peaks in the viscosity are also poorly understood, but may heuristically be associated with phase inversion. Thus on passing from oil-in-water microemulsion to bicontinuous phase there is a rather important change in the microstructure that must be reflected in the viscosity. Finally we note that near these viscosity peaks the microemulsion becomes non-Newtonian and undergoes shear thinning by factors of two to five at shear rates of 1000 s^{-1}.

It is worth remarking that, although there have been a number of other experiments in different parts of the phase-diagram that suggest that shear induces the reversible formation of new supermolecular structures, few systematic studies have yet appeared in the literature.

We also mention briefly some recent studies of the relaxation of microemulsion to equilibrium. Such relaxation processes appear to be well described by the Kohlrausch-Williams-Watts (KWW) exponential law, $\varphi(t) = A\exp\left\{-(t/\tau)^b\right\}$, where t, the characteristic relaxation time, and the parameter b are dependent on both temperature and the composition of the system. Recently however, López-Quintela and Losada reported a relaxation experiment on an oil-AOT-brine (3% NaCl solution) microemulsion that may be fitted by a KWW relaxation law with $b > 1$.

We intend to present two models[7] that rationalize most of the important basic features of microemulsion. They are both based on Hamiltonians or simple form of the interactions and may be viewed as near-microscopic. The predictions obtained from such theories result from true statistical mechanical calculations. The assemblies form and evolve spontaneously simply as a result of competition between the various energy and entropy effects. This permits one to calculate simultaneously the phase-diagram and the structural properties of these materials, thereby elucidating the relationship between the two. This aspect is particularly important when one does not possess a truly quantitative theory that can make direct contact with the experimental phase diagram.

3. THE WIDOM-TYPE MODEL OF MICROEMULSION

The Hamiltonian that we shall present is closely related to that of Widom, a model that had itself grown from earlier researches by Wheeler and Widom.[8] It differs only in the generalization of some of the interactions. As in Widom's original treatment,[8] we divide configuration space into cubes of side a and this, the microscopic distance in the formulation, is chosen to be the length of an amphiphile molecule. Arbitrary configurations of the oil (AA), water (BB) and amphiphile molecules (AB) are then assigned to this lattice, subject to the constraint that only like ends of different molecules be permitted to lie within any cube. Thus, each cube of configuration space is composed of only hydrophilic or hydrophobic material and any molecular configuration may therefore be represented by values of Ising variables at their centers. Evidently there exist no isolated amphiphiles in this model, so to each local configuration of a pair of amphiphile molecules we may assign an additional energy that is chosen with respect to a pair of parallel amphiphile molecules that lie side-by- side. This ultimately leads to an unfavorable energy both for bending of an isolated amphiphilic film, and for the touching of two such layers. However these terms, being based only on pairs of amphiphiles, necessarily treat edges and corners of the amphiphilic film on equal terms in that a corner energy is calculated as the sum of edge-energies. Since we conceive the microscopic origins of this energy scale to lie in the partial-free-energies of proximate amphiphile molecules that are surrounded by oil, water and possibly cosurfactant, one expects the interaction Hamiltonian to possess many-body terms. In particular, the bending of an amphiphilic film certainly has a potential energy contribution but there is also penetration of water (or oil) into the film that must be accounted for by the microscopic interaction parameters. It is, therefore, evident that such contributions would be different for edges and corners of the amphiphilic film, and thus, in principle, require independent energy parameters. We therefore choose as our basic interactions the parameters V_1-V_5, these corresponding to the energies of the local configurations that are given in Figure 3.

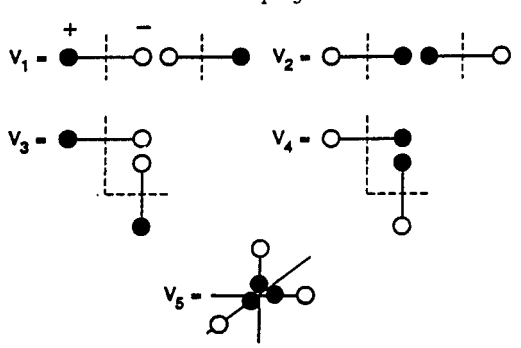

Figure 3. The molecular configurations of amphiphile that correspond to the interaction energies V_1-V_5. These energies are measured relative to that of a pair of parallel amphiphiles. The amphiphiles (AB) are represented by a hydrophobic (O) and hydrophilic (O) region and are considered to lie along the bonds of a simple-cubic lattice. The mid-points of every bond occupied by an amphiphile molecule collectively represent the amphiphilic film.

Note that the essential content of the foregoing arguments is that small regions or aggregates of amphiphile have only three basic significant energy scales *viz.*, the energies due to bends of an isolated film, these being distinct for edges and corners, and the energy of two proximate flat pieces of the film. For generality we must also differentiate between the ends of the amphiphiles, and this is reflected in the fact that the parameters V_1 and V_3 are different from V_2 and V_4.

Upon reflection we see that the lattice model really is simply a way of describing an ensemble of surfaces that can break and tear but that possess an energy of deformation. The coordinates of the surface are necessarily discrete, but for large aggregates the long length-scale properties are unaffected by this approximation.[9]

The centers of all cubes that compose configuration space define a regular cubic lattice. Since the interactions of figure 3 require knowledge only of a central and six surrounding cubes, one may construct the total energy from octahedral clusters of Ising spins. Each octahedron involves seven Ising variables, and we may represent the local energy as a function of these Ising spins. The energy of each of the twenty such octahedral fragments (see Figure 4) may be compiled from the rules in Figure 3. We then require that the chosen function of the Ising variables correctly reproduces the energies of all twenty local-spin configurations given in Figure 4.

It transpires that the local-energy contribution requires only one- to four-body spin interactions and the Hamiltonian may be written

$$\mathcal{H} = H\sum_{n}\sigma_n + \sum_{n,n'} J_{n,n'}\sigma_n\sigma_{n'} + \sum_{n,n',n''} L_{n,n',n''}\sigma_n\sigma_{n'}\sigma_{n''} + \sum_{n,n',n'',n'''} P_{n,n',n'',n'''}\sigma_n\sigma_{n'}\sigma_{n''}\sigma_{n'''} \qquad 3.1$$

The spin-interaction coupling constants refer to the interactions for isolated spins as well as those between pairs, triples and quadruples of spins. The two-body spin interactions $\{J_{n,n'}\}$ are nearest-neighbor (J), diagonal neighbor (M_1) and linear next-nearest-neighbour (M_2) and their definitions in terms of the elementary energies V_1-V_5 are given in Table 1.

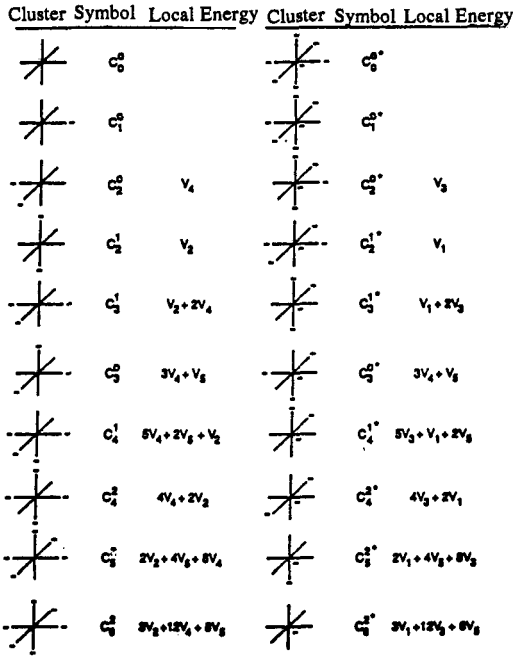

Figure 4. The energy of every local-octahedral Ising spin configuration. These values may be calculated using the definitions in Figure 1.

Table 1. Transcription from Ising variables to interaction energies and chemical potentials in the solution. The molecular configurations corresponding to the interaction energies V_1-V_5 are given in Figure 3.

Ising Variables	Microemulsion Model
H	$3/2(\mu_{BB} - \mu_{AA})$
J	$1/4V_2 - V_3 - 1/4(\mu_{AB}-(\mu_{BB}+\mu_{AA})) + 1/2V_5$
M_1	$-1/4(V_3 + V_5)$
M_2	$-1/8V_2$
P	$1/8V_5$

The early detailed studies of this model were confined to the choice of parameters M_1=M, M_2=2M, L_1=L_2=P=0. If one makes the choice H=L_1=L_2=0, corresponding to zero spontaneous curvature of the amphiphile film and equality of the chemical potentials of oil and water, one would expect to find the bicontinuous microemulsion to be one of the prominent phases. The Hamiltonian then becomes

$$\mathcal{H} = \tfrac{1}{2}\sum_{n}\sigma_n O_n\sigma_n + P\sum_{n,n',n'',n'''}^{4B}\sigma_n\sigma_{n'}\sigma_{n''}\sigma_{n'''} \qquad 3.2$$

$$O_n = a_4(\Delta_n^4) + a_2(\Delta_n^2) + a_0 \qquad 3.3$$

$$(\Delta_x^2)f_x = f_{x-1} + f_{x+1} - 2f_x \qquad 3.4$$

$$(\Delta_x^2) + (\Delta_y^2) + \Delta_z^2 = \Delta_n^2 \qquad 3.5$$

$$a_4 = -M \qquad 3.6$$

$$a_2 = -(J + 12M) \qquad 3.7$$

$$a_0 = -6(J + 5M) \qquad 3.8$$

where, to make connection with earlier researches, we set M_1=2M (M_2=M) and thus,

$$J = \frac{1}{2}\left(\mu_{AB} - \frac{1}{2}(\mu_{AA} + \mu_{BB})\right) - \frac{5}{2}K \qquad 3.9$$

$$M = -K/4 \qquad 3.10$$

where K was, in the original literature, referred to as the bending energy of the amphiphilic film.

For this set of restrictions one finds that the present model is equivalent to that of Widom, except for the presence of a four-body term that reflects the selection of an independent corner energy in Figure 3.

As it stands this is a model that can be studied using mean-field theory or Monte-Carlo simulation. In either case one may calculate the properties for different energy parameters (V_1-V_5) and as a function of the chemical potentials of oil, water and amphiphile. The results are presented in the form of phase-diagrams where one plots the phase-transition lines and phases that are stable in the various regions. The construction of such phase-diagrams are often the result of considerable effort and we will not enter into the details in the main text. The interested reader should consult reference 10 for a discussion of mean-field theory[10] and reference 11 for simulation and renormalization calculations. One cut of the complete phase diagram is presented in Figure 5.

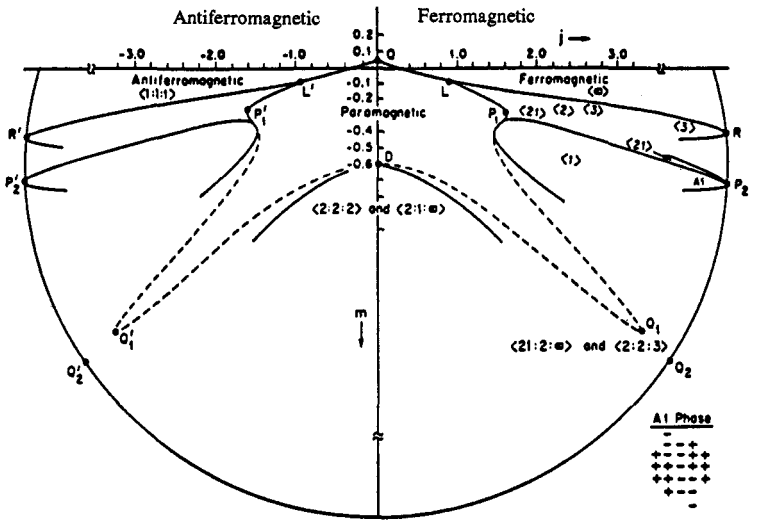

Figure 5. A cut (L_1=L_2=0, H=0, P=0, M=M_1,M_2=2M) of the lattice model composed from simulation, renormalization and other calculations (see reference 11).

This cut corresponds to equal chemical potentials for oil and water (H=0), zero spontaneous curvature of the film (L_1=L_2=0), P=0, and the choice M=M_1, M_2=2M. It should therefore be a cut where the bicontinuous microemulsion phase is prominent. In fact, since the microemulsion is spatially disordered we identify it with the disordered (or paramagnetic) phase of the spin-model. In another figure (Figure 6) we present a more schematic version of the extended model for P>0.

It should be noted that the densities of the components can always be reconstructed from the average values in the spin model. Thus, the density operators are,

$$\hat{\rho}^{AA}(\mathbf{n}) = \frac{1}{2}(1 + \sigma_{\mathbf{n}}) \qquad 3.11$$

$$\hat{\rho}^{BB}(\mathbf{n}) = \frac{1}{2}(1 - \sigma_{\mathbf{n}}) \qquad 3.12$$

$$\hat{\rho}^{AB}(\mathbf{n}, \hat{\mathbf{a}}) = \frac{1}{2}(1 - \sigma_{\mathbf{n}}\sigma_{\mathbf{n}+\hat{\mathbf{a}}}) \qquad 3.13$$

where $\hat{\mathbf{a}}$ is the orientation of the lipid (AB) molecule that lies between sites $\mathbf{n}$ and $\mathbf{n} + \hat{\mathbf{a}}(\hat{\mathbf{a}} = \hat{\mathbf{x}}, \hat{\mathbf{y}}, \hat{\mathbf{z}})$ These quantities are zero or unity depending on whether a molecule is present at site $\mathbf{n}$. The average densities are then just given simply by the averages $\langle \sigma_{\mathbf{n}} \rangle$ and $\langle \sigma_{\mathbf{n}} \sigma_{\mathbf{n}+\hat{\mathbf{a}}} \rangle$. Also, the fluctuations in these averages may also be calculated and compared to the results from neutron scattering. Thus, for example, for a bicontinuous microemulsion with equal volume fractions of oil and water $\rho^{AA} = \langle \hat{\rho}^{AA} \rangle$ is equal to

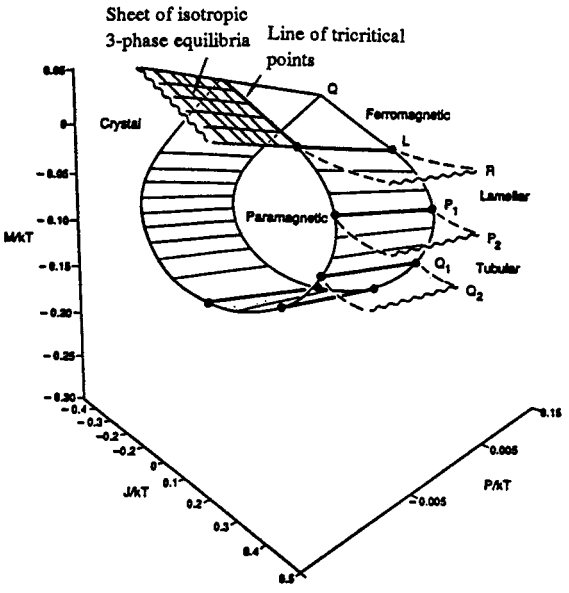

Figure 6. Phase-diagram in space of Ising-model couplings, j(=J/kT), m(=M/kT), P=(P/kT), for the range -1/96≤P≤0. The points Q, L, R, P_1, P_2, Q, Q_2 have been marked to provide a relation to the more detailed phase-diagram of reference 10. The paramagnetic phase is identified with isotropic mixtures of oil, water and amphiphile. In the vicinity of the curve L and in the interior of the capped elliptical cylinder the disordered phase takes on the properties of microemulsion.

$\rho^{BB} = \langle \hat{\rho}^{BB} \rangle (\langle \sigma_n \rangle = 0)$. In this case,

$$G^{AA/AA}(\mathbf{n}-\mathbf{n}') = \langle \delta\hat{\rho}^{AA}(\mathbf{n}) \delta\hat{\rho}^{AA}(\mathbf{n}') \rangle = \frac{1}{4}\langle \sigma_n \sigma_{n'} \rangle \qquad 3.14$$

where $\delta\hat{\rho} = \hat{\rho} - \langle \hat{\rho} \rangle$.

Using all of these relations it is possible to reconstruct the predictions for the amphiphilic solution from those of the equivalent Ising Model. Thus, for example, by computer simulation we can calculate the water-water correlation function. Examples are given in reference 11.

To make the Ising model a little bit simpler to understand and to pursue some analytical calculations we shall now make a continuum approximation that should describe long length-scales fairly well. This is achieved by making the "soft-spin" approximation and entails replacing the discrete Ising spins, for which $\sigma_n = \pm 1$, by a continuum "spin" variable, $\varphi(\mathbf{r})$ which may have any value between $\pm\infty$. We begin our study by constructing an effective LGW Hamiltonian.[12] To do this we perform a Hubbard transformation on the partition function of the Hamiltonian (3.2) with P=0. The result of this transformation is

$$Z = \sum_{\{\sigma_n\}} e^{-H} = \int D\varphi_n e^{-H(\varphi_n)} \qquad 3.15$$

$$D\varphi_n = \frac{1}{(\det L_n)^{\frac{1}{2}}} \prod_n \frac{d\varphi_n}{(2\pi)^{\frac{1}{2}}} \qquad 3.16$$

$$H = -\frac{1}{2}\sum_n \varphi_n O_n^{-1} \varphi_n - \sum_n \ln(2\cosh\varphi_n) \qquad 3.17$$

The LGW Hamiltonian is constructed by expanding the last term in equation 3.17 and keeping only the terms up to quartic order, since typically, all of the higher powers will be irrelevant to the study of near critical behavior of the theory. Transforming to Fourier space we see that the coefficient of the quadratic term is $-O_q^{-1} - 1$. We therefore define

$$K_q = O_q + 1 \qquad 3.18$$

Within the mean-field theory the phase-transition from the paramagnetic to the non-uniform phase with wave vector q_c occurs at $K_{q_c} = 0$ and $\nabla K_{q_c} = 0$.[12] Thus, close to the transition line we can expand in powers of K_q to obtain,

$$H = \tfrac{1}{2}\sum_q |\varphi_q|^2 K_q + \tfrac{1}{12}\sum_q \varphi_{q_1}\varphi_{q_2}\varphi_{q_3}\varphi_{q_4}\delta(q_1+q_2+q_3+q_4) \qquad 3.19$$

In this paper we shall concentrate our attention on that region of the phase-diagram in the vicinity of the Lifshitz point ($q_c = 0$). In this region it is possible to expand K_q in the powers of q to obtain,

$$K_q = b_0 + b_1 q^2 + b_3 q^4 + b_4 \sum_{i=1}^{3} q_i^4 \qquad 3.20$$

where,

$$b_0 = 1-6(j+5m) \tag{3.21}$$

$$b_1 = (j+12m) \tag{3.22}$$

$$b_3 = -m \tag{3.23}$$

$$b_4 = -\tfrac{1}{12}(j+12m) \tag{3.24}$$

and i=1,2,3 denotes the x,y,and z directions respectively. It is worth pointing out that the resulting form of the LGW Hamiltonian is believed to be the simplest possible for description of the bicontinuous phase and, therefore, in some sense is canonical. The scaling of the bare coupling constants with the microscopic energies and chemical potentials is an additional benefit of having begun with a lattice model.

Now the physical meaning of the term quadratic in momentum is evidently just a surface energy. We also note that the coefficient b, the effective bare tension, contains both an interaction term (m) and the relative chemical potential (j).[13] Therefore the bare tension may be chosen by adjusting molecular structure and concentrations independently. In this regard it is important to maintain the picture of the interface as one that is truly open to mass transfer, rather than a simple mechanical surface. The coefficient of the quartic term in momentum reflects both curvature and compression contributions, and will also serve to set the energy scale, while the φ^4 term is the leading effect of the excluded-volume interactions. Since, near the Lifshitz point, the cubic anisotropy is small we spherically average the last term in the equation (3.20). Finally normalizing the quartic term of (3.20) to $\frac{1}{2}$ we have the effective action

$$H = \frac{1}{2}\int_{\mathbf{q}} |\varphi_{\mathbf{q}}|^2 \left(q^4 + bq^2 + c\right) + \frac{\lambda}{4!}\int_{\mathbf{q}} \varphi_{\mathbf{q}_1}\varphi_{\mathbf{q}_2}\varphi_{\mathbf{q}_3}\varphi_{\mathbf{q}_4}\delta(\mathbf{q}_1+\mathbf{q}_2+\mathbf{q}_3+\mathbf{q}_4) \tag{3.25}$$

and

$$b = \frac{-20(j+12m)}{(j+32m)} \tag{3.26}$$

$$c = \frac{120(j+5m)-20}{(j+32m)} \tag{3.27}$$

$$\lambda = \frac{800}{(j+32m)^2} \tag{3.28}$$

We will use this action as a starting point for the analysis of the fluctuations.

We study the renormalization of the coupling constants within a modified Hartree approximation. The fully self consistent equation for the self energy is shown diagrammatically in figure 7 and may be written,

$$-\Sigma(\mathbf{p}) = \frac{\lambda}{2}\int G(\mathbf{q};\Sigma)\frac{d^3\mathbf{q}}{(2\pi)^3} + \frac{\lambda^2}{6}\int G(\mathbf{q};\Sigma)G(\mathbf{k};\Sigma)G(\mathbf{p}-\mathbf{q}-\mathbf{k};\Sigma)\frac{d^3\mathbf{q}}{(2\pi)^3}\frac{d^3\mathbf{k}}{(2\pi)^3} + O\left(\lambda^3\right) \tag{3.29}$$

$$G(\mathbf{q};\Sigma) = \frac{1}{\mathbf{q}^4 + b\mathbf{q}^2 + c - \Sigma(\mathbf{q})} \tag{3.30}$$

This equation corresponds to the resummation of the most divergent diagrams of the theory. We note that our choice of normalizing the coefficient of q^4 to $\frac{1}{2}$ is a calculational convenience and was not necessary. It is satisfactory if the coefficient of the quartic term in the expansion of $\Sigma(\mathbf{q})$ is small. Later we shall see that, typically, this is indeed the case.

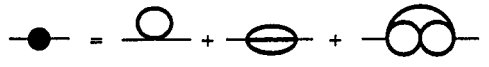

Figure 7. The self consistent equation for the self energy in the modified Hartree approximation. Here the bold faced lines denote the renormalized propagator, and the filled circle is the self-energy. The first two diagrams have been evaluated in Section 3. The final one ($O(\lambda^3)$) is discussed in reference 14.

The one-loop diagram , being momentum independent, will renormalize only the coefficient c, while the other diagrams will renormalize both the quadratic and quartic terms via the second and fourth derivatives of $\Sigma(\mathbf{q})$ in a Taylor expansion for small $\mathbf{q}$. That one may neglect the higher powers of $\mathbf{q}$ that are generated by renormalization and truncation of the self-consistent series at low orders in the evaluation of $\Sigma''(0)$ and $\Sigma''''(0)$ is an assumption that is difficult to justify rigorously,[15] though one can estimate the corrections by evaluation of one further order than that considered in the renormalization. However, on general grounds one can argue that the corrections are small. The interested reader should consult the original paper.[14]

Now the one-loop integral has been previously performed in equation (3.2). It is, however, more convenient to perform the two-loop integral in real-space,

$$\int G(q)G(k)G(p-q-k)\frac{d^3q}{(2\pi)^3}\frac{d^3k}{(2\pi)^3} = \int e^{ip\cdot r}G^3(r)d^3r \tag{3.31}$$

$G(r)$ is just a two-point function $\langle\varphi(0)\varphi(r)\rangle$ that can easily be obtained by contour integration to give

$$G(r) = K\frac{e^{-\frac{r}{\xi}}}{r}\sin\left(\frac{2\pi}{d}r\right) \tag{3.32}$$

where,

$$K = \frac{1}{2\pi(4c-b^2)^{\frac{1}{2}}} \tag{3.33}$$

$$\frac{1}{\xi} = \left(\frac{\sqrt{c}}{2}+\frac{b}{4}\right)^{\frac{1}{2}} \tag{3.34}$$

$$\frac{2\pi}{d} = \left(\frac{\sqrt{c}}{2}-\frac{b}{4}\right)^{\frac{1}{2}} \tag{3.35}$$

The renormalized c_r and b_r are given by

$$c_r = c - \Sigma(0) \tag{3.36}$$

$$b_r = b - \frac{1}{2}\Sigma''(0) \tag{3.37}$$

Here the prime stands for differentiation with respect to q. Inserting the above results into the self consistent equation (3.4) we obtain

$$b_r = b - \frac{\lambda^2}{4\pi^2(xy)^{\frac{3}{2}}}\left(\frac{(xy)^{\frac{1}{2}}}{(9x+y)^2} - \frac{(xy)^{\frac{1}{2}}}{81(x+y)^2}\right) \tag{3.38}$$

$$c_r = c + \frac{\lambda}{8\pi\sqrt{x}} + \frac{\lambda^2}{48\pi^2(xy)^{\frac{3}{2}}}\left(3\cot^{-1}3\left(\frac{x}{y}\right)^{\frac{1}{2}} - \cot^{-1}\left(\frac{x}{y}\right)^{\frac{1}{2}}\right) \tag{3.39}$$

where,

$$x = 2\sqrt{c_r} + b_r \tag{3.40}$$

$$y = 2\sqrt{c_r} - b_r \tag{3.41}$$

and b and c are the bare parameters given by equations (3.26) and (3.27). Note that b_r has a status of a renormalized surface tension, measured relative to the curvature contribution. We can solve these non-linear equations numerically for any given choice of bare couplings, b and c.

Note that the variation of d and ξ as a function of j and at fixed m is more meaningful in the interpretation of the Hamiltonian as a microemulsion model. By considering the transcription from coupling to solution-model constants[4,5]

$$\Delta\mu = -\frac{5}{2}\kappa + j \tag{3.42}$$

$$m = -\frac{\kappa}{4} \tag{3.43}$$

one sees that this choice amounts to fixed bending energy of the amphiphilic film (κ), and decreasing amphiphile concentration ($\Delta\mu$). Evidently d should increase, reflecting the increase in domain size. The mean-field theory of this is qualitatively incorrect, while the renormalized theory agrees qualitatively, with fair quantitative agreement. As an example (figure 8) we consider the cut m=-.048 for j between .5 and .66, a line that passes close to the renormalized Lifshitz region. The values of d increase , and in principle diverge as one crosses the Lifshitz point. The Monte-Carlo values of m=-.11, and j varying between .65 and .95 corresponding to a cut close to the Monte-Carlo Lifshitz point, is presented in figure 9 for comparison. Though there is a fair amount of scatter in the points reflecting both statistical fluctuations and sensitivity to fitting for small and large values of d, we note that both theory and simulation are in quite good qualitative agreement with such experimental values of d and ξ as a function of concentration as we possess.[16] However, as of yet no serious attempt has been made to fit a sequence of data using the recursion relations (3.13) and (3.14).

4. THE INTERFACIAL TENSIONS AND STRUCTURE OF THE INTERFACES BETWEEN PHASES IN THE LATTICE MODEL

Within the context of mean-field theory one may also construct the interfacial profiles and tensions between the various phases that are in equilibrium in the phase-diagrams, Figures 5 and 6. The interfacial tensions derived from such calculations are expected to be qualitatively correct.[17] One may also heuristically associate the mean-field profiles with the interfacial structure of small regions of the interface. As we shall see, the tensions calculated for the present lattice model are characteristically low, even when there is no proximate critical point. Thus, in the region of three-phase oil-water-lamellar-coexistence one finds that the oil-lamellar phase or

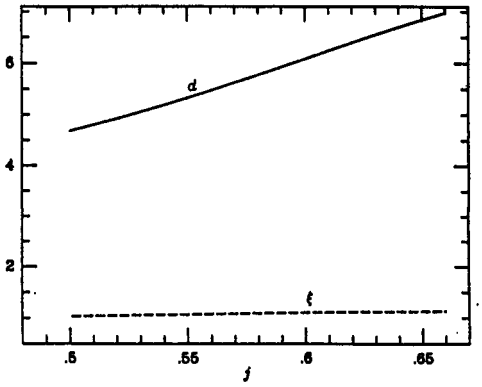

Figure 8. The renormalized d and ξ as a function of j with m held at a constant value of -0.048. This ray passes close to the predicted renormalized Lifshitz point.

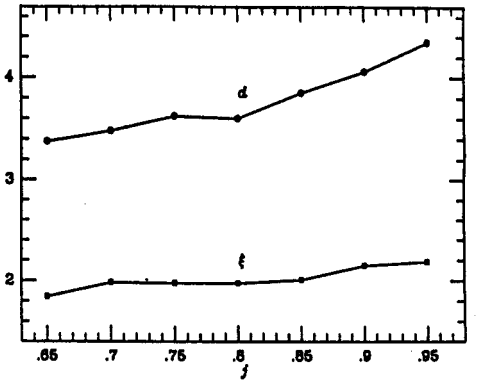

Figure 9. Monte-Carlo data for d and ξ as a function of j, with m held at a constant value of -0.11. This ray passes close to the Monte-Carlo predicted Lifshitz point.

water-lamellar phase tensions are all ultra-low (of order 10^{-4}kT). One also finds interfacial structure rather reminiscent of liquid-crystalline order at the interface between the oil-rich and water-rich phases.[18] In fact that this implies the existence of a non-trivial length-scale, besides the correlation length, at the interface between isotropic phases. The precise evolution of these length-scales as a function of the parameters of the model is readily determined numerically, or approximately by a perturbation theory based on the susceptibility of the isotropic phases. It is also worth noting that this phenomenon is intimately related to the peak in the scattering intensity that was discussed in the previous section. It is a prediction that has not yet been checked by experiments, though such studies are now becoming feasible. In the calculations presented below, in Figures 10-12, we plot the particle-density for each layer, z. These results are obtained by averaging the mean-field free-energy functional, over the x,y directions and then minimizing with the respect to the layer densities, subject to the asymptotic conditions for the two bulk phases that are in equilibrium.

In Figure 10 we plot a typical oil-water interface along the three-phase equilibrium surface between oil, water and lamellar phase. We note the symmetrical interfacial structure. Figure 11 corresponds to an oil-microemulsion interface that is on the three-phase

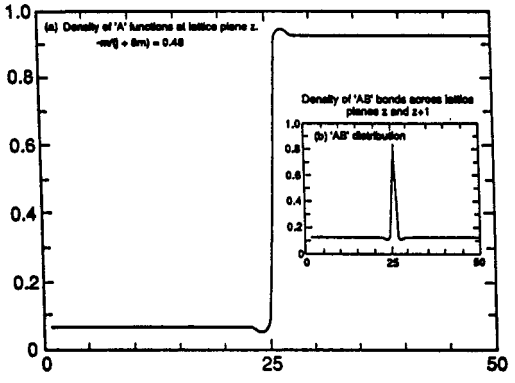

Figure 10. Typical density plot for oil-water interface for a point on the oil, water, liquid-crystal equilibrium surface. Note the presence of interfacial structure. On the inset we have presented the amphiphile density distribution across the interface. The interfacial tension corresponding to this profile is ultra-low.

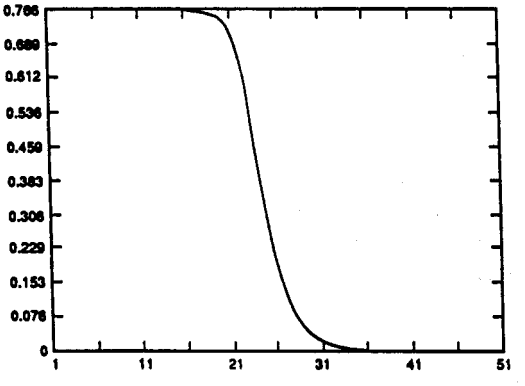

Figure 11. Typical oil-water interface for a point on the three-phase equilibrium surface between oil, water and isotropic phase, but far from the curve L.

equilibrium sheet, but somewhat away from the lamellar phases. For this reason the tension is still not extremely low, nor is there any discernible interfacial structure. Also, for these values of the parameters the oil-water interface is found to be wet by the third, microemulsion phase, a matter to which we shall return in some detail at the end of this section.

The next result, Figure 12, is derived for a point on the isotropic three-phase equilibrium surface that is much closer to the lamellar phase. Consequently, one might expect the appearance of interfacial structure. However, although the oil-water interface (not shown) is structureless, the oil-microemulsion or water-microemulsion (Figure 12) interface has structure, mainly confined to the microemulsion side. This is an observation that might be checked experimentally. One can show, in fact, that within the present model this particular type of interfacial structure is commonly associated with Winsor III equilibria and may, in some measure, be used to differentiate between these and conventional three-phase equilibria.

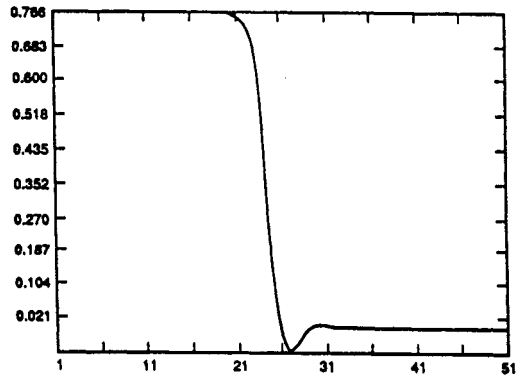

Figure 12. Typical microemulsion-water interface for a point on the three-phase equilibrium surface between oil, water and isotropic phase close to the curve L. At this point the isotropic phase possesses the features of a bicontinuous microemulsion and this is associated with structure in the microemulsion side of the interface.

At this point we may pause to review the origins of ultra-low interfacial tension, at least within the framework of the present lattice model. Actually, many of the important applications of amphiphilic dispersions stem from the remarkably low interfacial tensions found between the phases in the three-phase triangle, so this question has caused considerable interest and controversy in the literature. More recently it has become common to attribute the phenomenon to the near-cancellation of the bare surface-tension and the transverse component of the pressure.[19] There is both experimental[20] and theoretical[21] evidence that such effects are indeed significant. However, the predictions of the lattice model imply that the resolution to the question may not be so simple and that such cancellations lead to low, but not ultra-low, tension. To see that this is the case we recall that, because of the constraint that there are no direct oil-water contacts, all of the amphiphilic film satisfies the Schulman condition.[22]

We have, in addition, chosen the zero of energy to be that of flat amphiphilic film so that at any temperature the tension of a perfectly flat interface would be zero. This choice ensures that the conjectured condition for ultra-low tension is automatically satisfied by the construction of the lattice Hamiltonian. However, finite temperature effects cause fluctuations that disrupt and bend the interface in a number of ways and it thereby acquires an effective tension. This tension has been calculated for the three-phase equilibrium surface between oil-water and isotropic phase of Figure 6. The tension is low across most of the surface, but becomes ultra-low only near a tricritical point, or near the multistate surface from which the layered phases emerge. This multiphase surface had earlier been identified by requiring that the work required to insert an amphiphile into the film vanish. Note, therefore, that one appears to require this further constraint upon the microscopic parameters and chemical potentials of the model before the tensions become comparable to those that are conventionally called ultra-low. Given the integrity of the predictions of the model so far, one expects such a constraint must also be satisfied by experimental systems with ultra-low tension, an observation which could readily be evaluated experimentally. In fact, as we shall see later, the picture offered by the microemulsion model leads one to suppose that the practical rules-of-thumb at present used to predict ultra-low tensions are actually a reflection, albeit an imprecise one, of the constraints implied by the present model. We note finally that, since this explanation of the origin of ultra-low tension does not require proximity to any critical point, there is no implication that the compositions of the three phases should be nearly the same. In fact, typically the three-phase Winsor III equilibrium in this model are far from being critical when one considers compositions of the components. This point is important since it rationalizes some of the apparently conflicting observations on these systems that were mentioned in the introduction of the paper. This point is connected to another puzzling observation; thus the oil-water interface of a Winsor III state is typically non-wet by the microemulsion,[23] though there has been at least one observation of a transition to wetting.[24]

In the calculations described above one notes that for values of the parameters near the multistate surface, and consequently for a structured interface, the oil-water interface is not wet by the microemulsion phase. We may pursue the issue of wetting across the Winsor progression somewhat more systematically using mean-field calculations of the type described above. In this case, however, one must study the phase-diagram as a function of the coupling constants H and L that break the inversion symmetry. This permits us to locate the critical-end-points that bound the Winsor progression. These parameters involve, respectively, the difference in chemical potentials of oil and water and the spontaneous curvature of the amphiphilic film. These quantities in turn reflect the changes in the concentration of oil and water and in the amount of brine or cosurfactant present in the system. For ionic surfactants the Debye screening induced by the addition of salt can significantly affect the propensity of the amphiphilic film to bend toward water regions, thereby reducing the magnitude and removing the symmetry in the edge and corner energies of the lattice model. For our purposes it is important to note that most of the freedom present in the parameter space of the Hamiltonian is removed if one chooses to study such phase equilibria. The interfacial tensions and contact angles measured for these phase equilibria are dependant on relatively few or none of the parameters of the model. This is a useful consistency check on our understanding of the meaning of the microscopic parameters in the model.

We examine the surface of isotropic three-phase equilibria of the symmetric model. The three interfacial tensions may be computed and a curve of wetting transitions determined (see Figures 13 and 14). To one side of the curve w(j,m,P) $\left(\mathcal{P} = \frac{P}{kT}\right)$ the isotropic

Figure 13. The sheet of isotropic three-phase equilibria in space of parameters j, m, P. Above the surface one has the oil and water micellar phases and beneath it the isotropic phase. In the vicinity of the curve L the isotropic phase possesses the properties of micro-emulsion. Note that on the shaded portion of the surface the oil-water interface is not wet by the isotropic (microemulsion) phase. The curve w(j,m,P) thus represents a curve of second-order wetting transitions. The curve L and W are fairly close together so, in accordance with most experimental observations, we conclude that microemulsion tends not to wet the oil-water interface.

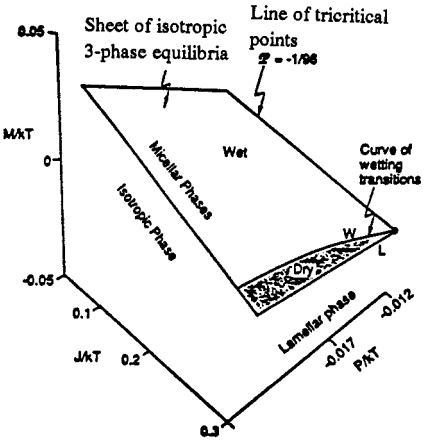

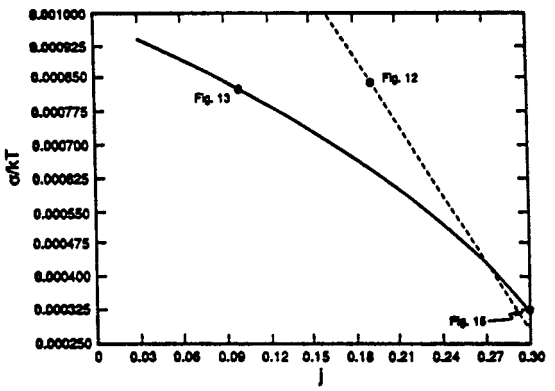

Figure 14. Location of a wetting transition for oil-water interface. The broken line is $2\sigma_{ow}$, whilst the full curve is $\sigma_{\mu w}$. At the crossing the microemulsion wets the oil-water interface. The points marked on the curves indicate the figures where density profiles for those values of the parameters have been presented.

surfactant-rich phase wets the oil-water interface. On the other side (shaded) the oil-water interface is non-wet, as might be expected of a microemulsion. Note that, as one proceeds to the line of tricritical points, the extent of the region for which the interface is non-wet shrinks, reflecting the normal trend that wetting accompanies the vanishing of interfacial tensions near a tricritical point. However, there is a novel phenomenon present in the lattice model of microemulsions. The interfacial tensions become small as one proceeds in either of two directions on the equilibrium sheet. Thus, as P becomes small the tensions vanish as one approaches the line of tricritical points. However, for fixed P the tension also becomes small as one approaches the multistate sheet (or tends to the curve L) because, as we have explained, the work for inserting an amphiphile molecule into the amphiphilic film is vanishing. This second mechanism for lowering the tensions is entirely unrelated to near-criticality and therefore carries with it no implication that the interface should be wet nor that the volume fractions of the components in different phases should be the same. On the contrary, the contact angles actually increase with decreasing oil- and water - microemulsion tensions. One can readily see that the issues of wetting, low interfacial tensions and near-criticality, (as determined by the volume fractions of the. components), are subtle and potentially confusing if one does not understand the global nature of the phase-diagram. Presumably the most common three-phase equilibria that are called Winsor III states are those that lie inside the non-wet region of the equilibrium surface. In some cases they may also be proximate to a tricritical point, reflecting a small corner energy term. Also, in some experiments one is probably close to both of the critical end-points, a matter to which we shall presently return. In either case the tensions would be lowered as a consequence of being close to a critical region we have mentioned. However, it is probable that the dominant effect in lowering the tension is proximity to the multistate surface, rather than any of these critical points. The interface would then be non-wet because the third phase, whether it be liquid-crystal or microemulsion, always has a higher tension with oil or water than in the case of critical wetting.

Though this phenomena has been reproduced with numerical calculations, it is also useful to develop a more intuitive understanding The tensions between all of these interfaces are quite low at low temperatures and, for the case of the oil-water interface, is significantly modified only by the in-layer fluctuations of the interface. However, the tensions with the lamellar phases or microemulsion are also affected by the fact that the principal fluctuating layer that defines the interface is hindered by the other amphiphilic films in the middle phase. This observation is closely related to the fact that there is a second, well-characterized length-scale (d) present in the lamellar and bicontinuous phases, *viz*., the average distance between the layers. As a consequence, these interfacial tensions tend to be higher than those between the simple oil-water interface where one has only micelles on either side of the interface. This means that if the third phase is sufficiently structured, that is, contains sufficient flat amphiphilic film then it will tend to form a lens rather than spreading out to wet the oil-water interface. Thus, even though all the interfacial tensions may be becoming lower on approach to the multistate surface, the amphiphilic film within the bicontinuous phase is becoming more flat and has a greater tendency to damp the interfacial fluctuations of the principal amphiphilic monolayer that defines the interface.

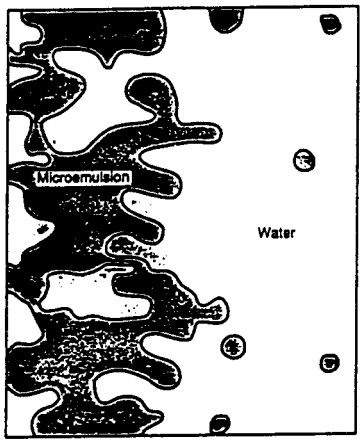

Figure 15. An instantaneous configuration from a Monte-Carlo simulation of the bicontinuous microemulsion-water interface. This calculation was carried out for a point on the three-phase equilibrium surface represented by figure P. Notice the degree of roughness of the interface, a phenomenon that would not be present for aa simple liquid-gas interface. The structure in the microemulsion side of the interface that was apparent in the mean-field calculations (figure 15) arise from the large domains that aggregate behind the principal amphiphilic film. Note carefully that this particular point was located using Monte-Carol simulation. It thus represents an interface at the Winsor III phase-equilibrium.

Furthermore the propensity of the middle phase to wet the oil-water interface is to a large degree determined by the lengths ξ and d since these determine the degree to which the principal monolayer is hindered. Finally in Figure 15 we have presented an instantaneous simulation configuration of an interface between water-rich and microemulsion phases. This example is presented to give a qualitative impression of the water-bicontinuous microemulsion interface at the Winsor III state. The configuration was prepared by first locating the Winsor III equilibrium by Monte-Carlo simulation of the heat-capacity and energy. An initial condition for the interfacial simulation was then constructed by filling half of the cube with equilibrated microemulsion and half the cube with an equilibrated water configuration. Average-structure von Neumann boundary conditions are then applied and the simulation re-equilibrated. However, we note that the interface is much more rough than one would expect from liquid-gas interface. In addition there is a tendency for large micellar aggregate to form on the microemulsion side, this being reflected in the mean-field density profile of Figure 12.

Note that we can now understand one more of the interrelations between experimental observations. Thus the condition that results in low tensions by stabilizing large amounts of flat amphiphilic film also results in a non-wet oil-water interface.

Such relationships may mean that the different attempts in the literature to resolve between classical three-phase equilibria and the Winsor III state for oil-, water- and bicontinuous-microemulsion are quite closely connected, even if they are not in quantitative agreement. This issue of how one should distinguish microemulsion is an interesting matter, and we shall return to it in the conclusions to this paper.

We now return to the general topic of interfacial tensions in the Winsor III three-phase equilibrium. In particular we wish to establish the idea that the present lattice model is capable of reproducing the characteristic pattern of tensions to which we referred in the introductory section of this paper. One would certainly expect this to be so since, as we have previously commented, the extended parameter space contains the oil-microemulsion and water-microemulsion critical-end-points. In addition, we know that the symmetric model ($H=L_1=L_2=0$) that contains the bicontinuous microemulsion phase possesses a region of non-wet three-phase equilibria. The essential ingredients of the interfacial tension plots are, therefore, already present. In Figures 16-18 we have presented calculations of the oil-water (σ_{ow}) oil-isotropic phase ($\sigma_{o\mu}$) and water-isotropic phase ($\sigma_{w\mu}$) tensions between the critical end-points.

In the absence of any constraints beyond those implied by the phase equilibria it is possible to choose an arbitrary relationship between j and m. This will in turn select a trajectory that, for the symmetric three-phase condition ($l_1=l_2=h=0$) corresponds to a point on the three-phase equilibrium sheet. We therefore present three plots for j+11m=0 (Figure 16), j+12m=0 (Figure 17), j+13m=0 (Figure 18) these corresponding respectively to oil-water interfaces that are dry, undergoing a wetting transformation, and wet by isotropic phase. Recall also that the isotropic phase tends to have the properties of microemulsion only for the first two choices of the j, m

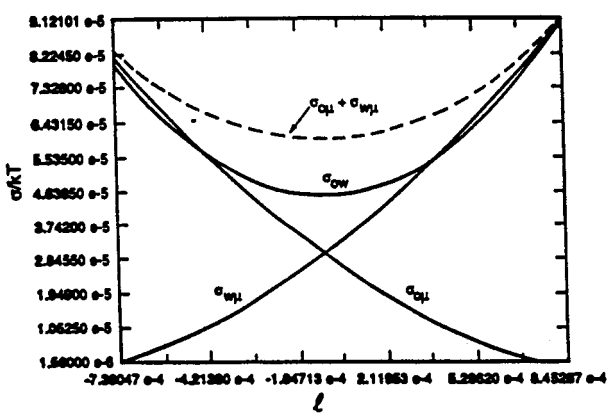

Figure 16. The interfacial tensions across the Winsor progression. The left-hand and right-hand-sides correspond respectively to water-microemulsion and oil-microemulsion critical end-points. This particular trajectory (j+11m=0) crosses the three-phase surface (figure 16) to the right of the wetting curve so the oil-water interface is not wet by isotropic phase. Also, since we are close to the curve L, the isotropic phase possesses the properties of microemulsion. These predictions are all in accord with experimental observation.

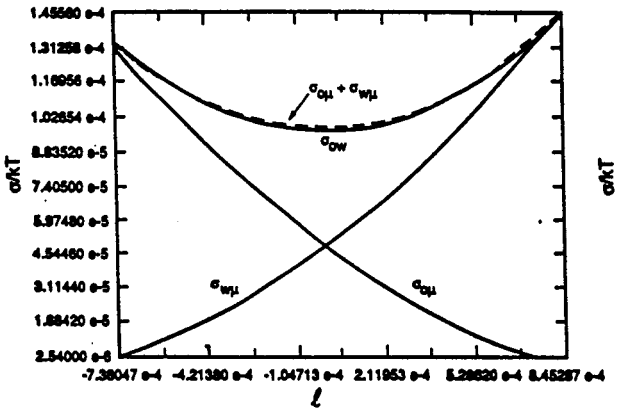

Figure 17. The interfacial tensions across the Winsor progression. (Note that $\ell = \frac{L}{kT}$, $L=L_1=L_2$). The left-hand and right-hand-sides correspond respectively to water-microemulsion and oil-microemulsion critical end-points. This trajectory (j+12m=0) crosses the three-phase surface (figure 16) very close to the wetting curve so the oil-water inter face is almost wet by isotropic phase. Also, since we are fairly close to the curve L, the isotropic phase still possesses the properties of microemulsion. Indeed, this may be viewed as a marginal microemulsion (see section 4).

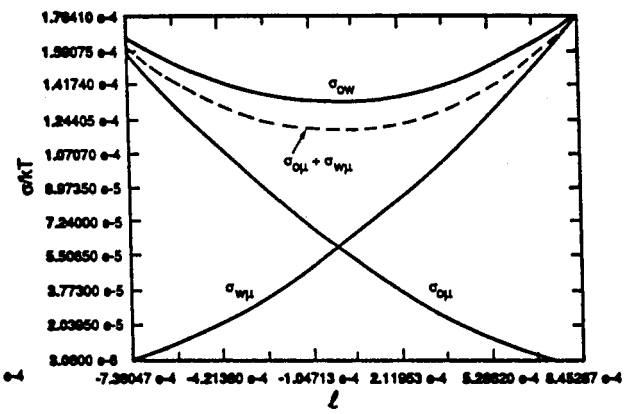

Figure 18. Here the isotropic phase wets the oil-water interface. Such a transition has recently been confirmed by various researchers (see, for example, reference 24).

relation, these being quite close to the curve L of Figure 6. The oil-water interface is non-wet for the first case (j+11m=0), in accordance with the experimental observation that, generally, Winsor III oil-water interfaces are not wet by microemulsion. It would in principle, be possible to make another selection that would produce a wet interface. It should be noted that, although the Winsor III interface is typically non-wet, a transition to wetting has been observed in at least one case. Such a situation is possible in the present model, but one would then predict that the peak in the S.A.N.S. data would move to smaller wave number. It would be interesting to check these ideas with measurements of tensions and of S.A.N.S. experiments.

In summary then, we have observed that Winsor III states tend to have non-wet oil-water interfaces because of the proximity to the multiphase sheet. Also, for Winsor III states, there are peaks in the experimental S.A.N.S data and these tend to occur at small wave-number. Similarly, in the present model one finds that as one proceeds along the three-phase surface towards the multiphase sheet one begins to see the emergence of a second length-scale in bulk and interfacial properties, this reflecting the proximity of an ordered phase on the phase-diagram. The two phenomena described above, the general absence of a tendency to wet and a secondary length scale, are related in the present model and, we believe, in the experiments. Thus, in this section we have commented that the flattening of the amphiphilic film causes the oil-water interface to be non-wet whereas, in our discussions of the correlation function we have shown that this same aspect is accompanied by a second length scale in the structure factor.

Having established the capacity of the model to describe these phenomena we may now turn to a rather old but practical question about the nature of an "optimal" microemulsion. In early experimental studies it was realized that a number of technologically important features of microemulsion are associated with the minimum in the oil-water interfacial tension that is found in the symmetric bicontinuous portion of the Winsor III state. From the arguments above, one may establish an understanding of the origins of this minimum in the oil-water tension. This permits us to establish to correspondence of microscopic interactions to the classical definition of an optimal microemulsion. However, in the space of parameters of this model there exists other degrees of freedom that might be exploited in establishing a more refined definition. A number of such questions have yet to be studied.

Acknowledgements The author wishes to acknowledge the contributions of John Gunn, Yan Levin, Michael McCallum, and Chris Mundy who participated in much of the work presented here. During the period that these ideas were developed the author benefitted much from conversations with Professor B. Widom who first introduced me to the study of microemulsion. Numerous other helpful insights were gained from conversations with Professor N. Boden, Professor S.-H. Chen, Professor M.E. Fisher, and Dr. M.D. Lipkin. The manuscript benefitted much from the advice and encouragement of Professor S. S. Elberg. Financial support in the early days of the research was provided by the Dreyfus and Sloan Foundations.

REFERENCES

1. The term is something of a misnomer, the molecules form large clusters or aggregates simply because of the particular balance of molecular energies.
2. Amphiphile from Greek roots amphi = both ends, philios = to love.
3. This aspect of these systems renders the self-avoiding surface models largely inapplicable to these situations.

4. Sometimes more than the three components, oil, water and amphiphile are added. Such components as salt or alcohol are termed cosurfactants and modulate the emulsion properties.

5. We emphasize that this is a *highly* schematic version of the phase diagram that is useful for theorists. Real phase-diagrams are considerably distorted from this picture. However, it is at present believed that these distortions arise from the fact that the solvent properties vary as a function of temperature. This diagram is from an article by H. T. Davis, J. F. Bodet, L. E. Scriven and W. G. Miller, on "Microemulsions and their Precursors," in *Physics of Amphiphilic Layers*, J. Meunier, D. Langevin and N. Bociara, Spring-Verlag Proceedings in Physics 21 (1987).

6. The notation $2\overline{3}2$ have been used by some to designate the progression from oil-microemulsion to water-microemulsion two (2) phase equilibria via the Winsor three-phase equilibrium. S.-H. Chen, S. L. Chang, R. Strey, J. Saniseth, and K. Mortensen, *Structural Evolution in Bicontinuous Microemulsions, an invited paper at the International Conference on Neutron Scattering*, Bombay, India, Jan. 21-25, 1991, to be published in proceedings.

7. One of these (the Ising Model) is more tractable for analytical calculations. The other is more flexible in that it may be extended to become a cellular automaton, thereby describing dynamical phenomena.

8. B. Widom, *Lattice Model of Microemulsions*, J. Chem. Phys. **84**, 6943 (1986) and earlier references therein. In particular, J. C. Wheeler and B. Widom, *Phase Transitions and Critical Points in a Model Three Component System*, J. Am. Chem. Soc. **40**, 3064 (1968); see also, K. A. Dawson, M. D. Lipkin, and B. Widom, *Phase Diagram of a Lattice Microemulsion Model*, J. Chem. Phys. **88**, 5149 (1988); B. Widom, K. A. Dawson, and M. D. Lipkin, *Hamiltonian and Phenomenological Models of Microemulsions*, Physica **140A**, 26 (1986). Other lattice and phenomenological models often give a similar description of many of these amphiphilic properties. The following, and the references therein, are representative: M. W. Matsen and D. E. Sullivan, Phys. Rev. A **41**, 2021 (1990); A. Ciach and J. S. Høye, J. Chem. Phys. **90**, 1222 (1989); A. Ciach, J. S. Høye, and G. Stell, J. Chem. Phys. **90**, 1214 (1989), J. Phys. A **21**, L777 (1988); J. W. Halley, J. Chem. Phys. **88**, 3313 (1988); M. Kahlweit and R. Strey, Langmuir **4**, 499 (1988); G. M. Garneiro and M. Schick, J. Chem. Phys. **89**, 4638 (1988); T. P. Stockfisch and W. H. Shih, J. Phys. Chem. **92**, 3292 (1988); K. Chen, C. Ebner, C. Jayaprakash and R. Pandid, Phys. Rev. A **38**, 6240 (1988), J. Phys. C **20**, 1361 (1987); M. Schick and W. H. Shih, Phys. Rev. Lett. **59**, 1205 (1987); A. Robledo, Phys. Rev. A **36**, 4067 (1987), Europhys. Lett. **1**, 303 (1986); D. Andelman, M. E. Cates, D. Roux, and S. A. Safran, J. Chem. Phys. **87**, 7229 (1987); S. A. Safran, D. Roux, and D. Andelman, Phys. Rev. Lett. **57**, 491 (1986); M. Schick and W. H. Shih, Phys. Rev. B **34**, 1797 (1986).

9. Any interface in a lattice model possesses a "roughening" temperature above which is fluid-like, beneath which it is "flat" or crystalline-like. It is easy to prove that, above the roughening temperature, the lattice interface Hamiltonian is equivalent to a fluid Hamiltonian. In our discussions of microemulsion, the interface will always be a rough one, so the effects of the lattice on long length-scale properties are probably negligible. See, for example, Y. Levin and K. A. Dawson, *Sine-Gordon Renormalization of the Orientational Roughening Transition*, Phys. Rev. A **42**, 3507 (1990). We should note, however, that such arguments are only technically valid for surfaces that do not deviate much from being planar. The large deviation case is not well understood.

10. K. A. Dawson, *Spatially Frustrated Lattice Models*, Phys. Rev. A **36**, 3383 (1987).

11. K. A. Dawson, B. L. Walker, and A. Berera, *Accounting for Fluctuations in a Lattice Model of Microemulsions*, Physica A **165**, 320 (1990).

12. K. A. Dawson, M. D. Lipkin, and B. Widom, *Phase Diagram of a Lattice Microemulsion Model*, J. Chem. Phys. **88**, 5149 (1988); K. A. Dawson, *Spatially Frustrated Lattice Models*, Phys. Rev. A **36**, 3383 (1987).

13. B. Widom, *J. Chem. Phys.* **84**, 6943 (1986); K. A. Dawson, M. D. Lipkin, and B. Widom, *Phase Diagram of a Lattice Microemulsion Model*, J. Chem. Phys **88**, 5149 (1988); K. A. Dawson, *Spatially Frustrated Lattice Models*, Phys. Rev. A **36**, 3383 (1987).

14. Y. Levin, C. J. Mundy, and K. A. Dawson, *Renormalization of a Landau-Ginzburg-Wilson Theory of Microemulsion*, Phys. Rev. A, in press.

15. S. A. Brazovskii, Sov. Phys. - JETP **41**, 85 (1978).

16. S. A. Chen, S. L. Chang, R. Strey, J. Samseth, K. Mortensen, *Structural Evolution of Bicontinuous Microemulsion*, (preprint); S.-H. Chen, S.-L. Chang, and R. Strey, *J. Chem. Phys.* **93**, 1907 (1990); E. W. Kaler, K. E. Bennett, H. T. Davis, and L. E. Scriven, J. Chem. Phys. **79**, 5673 (1983); H. Saito and K. Shinoda, J. Colloid Interface Sci. **102**, 647 (1970); C. Cabos and P. Delord, J. Appl. Cryst. **12**, 502 (1979); M. Kolarchyk, S.-H. Chen, J. S. Huang, and M. W. Kim, Phys. Rev. A **29**, 2054 (1984); M. Kolarchyk, S.-H. Chen, J. S. Huang, and M.W. Kim, Phys. Rev. Lett. **53**, 941 (1984); B. H. Robinson, C. T. Toprakcioglu, J. C. Dore, and P. Chieux, J. Chem. Soc. Faraday Trans. 1 **80**, 13 (1984); S.-H. Chen, T. Lin, and J. S. Huang, *Physics of Complex Supermolecular Fluids*, Exxon Monograph, S. A. Safran and N. A. Clark, Eds., Wiley and Sons, New York (1987).

17. K. A. Dawson, B. Walker, and A. Berera, *Accounting for Fluctuations in a Lattice Model of Microemulsions*, Physica A **165**, 320 (1990).

18. See, for example, A. Berera and K. A. Dawson, *Low Temperature Analysis of Three-Phase Coexistence*, Phys. Rev. Lett. **42**, 3618 (1990); K. A. Dawson, *Interfaces Between Phases in a Lattice Model of Microemulsions*, Phys. Rev. A **35**, 1766 (1987).

19. A. M. Cazabat, D. Langevin, J. Meunier and A. Pouchelon, *Critical Behavior in Microemulsions*, Adv. Colloid Interface. Sci. **126**, 175 (1982); R. Aveyard, B. P. Binks, S. Clark and J. Mead, *Interfacial Tension Minimum in Oil-Water-Surfactant Systems*, J. Chem. Soc. Faraday Trans. **82**, 125, (1986); J. R. Gunn and K. A. Dawson, *Microscopic Model of Amhiphilic Assembly*, J. Chem. Phys. **91**, 6393 (1989).

20. D. Guest, D. Langevin, and J. Meunier, *Liquid Interfaces: Role of the Fluctuations and Analysis of Ellipsometry and Reflectivity Measurements*, J. Phys. (Paris). **48**, 1819 (1987).

21. J. R. Gunn and K. A. Dawson, *Microscopic Model of Amhiphilic Assembly*, J. Chem. Phys. **91**, 6393 (1989).

22. T. P. Hoar and J. H. Schulman, Nature **152**, 102 (1943); J. H. Schulman, W. Stockenius, and L. M. Prince, *Mechanism of Formation and Structure of Microemulsion by Electron Microscopy*, J. Phys. Chem. **63**, 1677 (1959); see, for instance, H. F. Eicke and J. Rehak, *On the Formation of Water/Oil-Microemulsion*, Helv. Chim. Acta **59**, 2883 (1976).

23. That the interface is typically non-wet is indicated by, for example, H. Kunieda and K. Shinoda, *Correlation Between Critical Solution Phenomena and Ultralow Interfacial Tensions in a Surfactant/Water/Oil System*, Bull. Chem. Soc. Jpn. **55**, 1777 (1982).

24. J. van Nienwkoop and G. Snoei, Shell Research B.V., report No. 674 (January 1983), unpublished; M. Kahlweit, R. Strey, M. Aratono, G. Busse, J. Jen, and K. V. Schubert, *Tricritical Points in H_2O-Oil-Amphiphile Mixtures*, J. Chem. Phys. **95**, 2842 (1991); M. Aratono and M. Kahlweit, *Wetting in Water-Oil-Nonionic Amphiphile Mixtures*, J. Chem. Phys., submitted; M. Kahlweit and H. Reiss, *On the Stability of Microemulsions*, Langmuir, submitted.